Rhodium Nanoparticles

DOI: 10.1002/anie.200503174

Synthesis, Stability, and Surface Plasmonic Properties of Rhodium Multipods, and Their Use as Substrates for Surface-Enhanced Raman Scattering**

*Nobuyuki Zettsu, Joseph M. McLellan, Benjamin Wiley, Yadong Yin, Zhi-Yuan Li, and Younan Xia**

Controlling the shape of nanocrystals is critical to modern materials chemistry because the intrinsic properties of most nanomaterials are strongly dependent on their shape.[1] Tripod and tetrapod shapes have recently attracted much attention owing to their potential use as building blocks in the fabrication of complex, multiple-terminal devices through self-assembly.[2] Multipods made of type II–VI semiconductors, such as CdSe,[3] CdS,[4] and CdTe[5], have been known for several years. A key parameter for growing multipods of these solid materials is the energy difference between the zinc blend and wurtzite structures at certain temperatures, as one structure may be preferred during nucleation and the other during growth.[5] As most metals only exist in one crystal structure (often in the face-centered-cubic lattice), it is more challenging to grow branched nanocrystals from metals;[6] it

[*] Dr. N. Zettsu, J. M. McLellan, Prof. Y. Xia
Department of Chemistry
University of Washington
Seattle, WA 98195-1700 (USA)
Fax: (+1) 206-685-8665
E-mail: xia@chem.washington.edu

B. Wiley
Department of Chemical Engineering
University of Washington
Seattle, WA 98195 (USA)

Dr. Y. Yin
The Molecular Foundry
Lawrence Berkeley National Laboratory
Berkeley, CA 94720 (USA)

Prof. Z.-Y. Li
Laboratory of Optical Physics
Institute of Physics
Chinese Academy of Sciences
Beijing 100080 (P.R. China)

[**] This work was supported in part by a grant from the NSF (DMR-0451788) and a fellowship from the David and Lucile Packard Foundation. Y.X. is a Camille Dreyfus Teacher Scholar (2002). N.Z. was partially supported by a research fellowship from the Japan Society for the Promotion of Science (JSPS). B.W. thanks the Center for Nanotechnology at the UW for a fellowship. Z.-Y.L. was supported by the National Key Basic Research Special Foundation of China (Grant No. 2004CB719804). This work used the Nanotech User Facility (NTUF), a member of the National Nanotechnology Infrastructure Network (NNIN) funded by the NSF. We thank the Molecular Foundry at the Lawrence Berkeley National Laboratory for the HRTEM analysis.

Supporting information for this article is available on the WWW under http://www.angewandte.org or from the author.

will be very difficult at least, if not impossible, to achieve branched growth by means of structural transformation between the nucleation and growth steps. Nevertheless, a number of noble metals including Au,[7] Pt,[8] and Rh[9] have recently been demonstrated to form branched nanocrystals. The use of a capping agent such as cetyltriethylammonium bromide (CTAB) or poly(vinyl pyrrolidone) (PVP) is imperative, however, and this is probably just one of the prerequisites for achieving a branched morphology. The growth mechanism is yet to be completely understood for these systems.

Herein, we report the synthesis of Rh multipods as well as their stability, surface plasmonic properties, and use as substrates for surface-enhanced Raman scattering (SERS). Toshima and co-workers first reported their observation of branched Rh nanocrystals in the late 1970s.[9a] Most recently, Tilley and co-workers reported the polyol synthesis of Rh multipods and proposed a mechanism based on homogenous nucleation and seeded growth to account for the anisotropic growth.[9b] However, neither of these reports described any appealing properties associated with the Rh multipods. We also note that in both cases, the arms of the branched nanostructures were rather short, which could possibly be related to the involvement of water in the reaction media.[10] Here, we demonstrate that Rh multipods can be synthesized in high yields when anhydrous Na_3RhCl_6 (rather than $RhCl_3{\cdot}n\,H_2O$) is used as a precursor of Rh. We also report that the branched morphology can only prevail when oxygen is excluded from the reaction system. Otherwise, oxidative etching and Ostwald ripening would transform the branched nanocrystals into spheres in an effort to minimize the total surface energy.

The branched Rh nanocrystals were synthesized through a polyol process. In a typical procedure, Na_3RhCl_6 and PVP were separately dissolved in ethylene glycol and the two solutions were injected simultaneously into ethylene glycol (preheated to 140 °C) by a syringe pump. The color of the solution rapidly turned from rose pink to dark brown within 1 min, indicating the formation of Rh nanocrystals as $RhCl_6^{3-}$ was reduced by ethylene glycol. The as-obtained Rh nanocrystals were characterized using transmission electron microscopy (TEM). Figure 1 shows TEM images taken from a series of samples that were prepared by increasing the reaction time from 5 min to 48 h. In the initial stage of the reaction (Figure 1a and b), the particles exhibited a well-defined, branched morphology with three (tripod) or four (tetrapod) arms. Among them, tripods were in the majority, comprising approximately 70% of the total particle population. The arms were roughly 11 nm long at $t = 10$ min, but the apparent arm size varied slightly as a result of the difference in their orientation on the TEM grid. High-resolution TEM (HRTEM) studies clearly showed that the same fringe pattern continuously extended throughout each branched nanocrystal, suggesting the formation of a single crystal (Figure 1c). The interplanar distance was measured to be 0.22 nm. This value could be assigned to the spacing between {111} planes, implying that the arms grew in the ⟨111⟩ directions. Powder X-ray diffraction (XRD) patterns (see Supporting Information) of the as-prepared Rh multipods exhibited three peaks

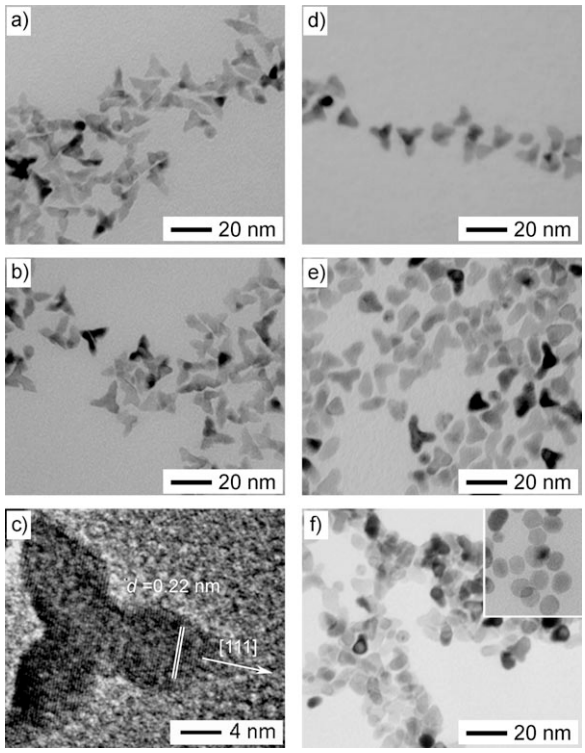

Figure 1. TEM images of Rh nanocrystals synthesized in air at 140 °C for different periods of time: a) 5 min; b) 10 min; c) 10 min (HRTEM image); d) 90 min; e) 6 h; and f) 48 h. The inset in (f) shows a TEM image of the sample at $t = 120$ h.

in the range $35° < 2\theta < 80°$ which correspond to the (111), (200), and (220) diffractions from face-centered-cubic Rh (JCPDS #05-0685).

As the reaction continued (Figure 1d and e), the overall length-to-width aspect ratio of the arm decreased as compared to the sample shown in Figure 1b. The branched Rh nanocrystals slowly evolved into rice-shaped particles at $t =$ 48 h and eventually became spheres at $t = 120$ h. The overall size of the nanocrystal also decreased in this process. The transformation from the branched shape into a spherical one could be interpreted in terms of oxidative etching and Ostwald ripening. Like other face-centered-cubic metals, the surface energy of Rh decreases in the order of (110), (100), and (111).[11] In an effort to minimize the total surface energy, the arm was slowly etched from the tip and the resultant Rh ions were reduced and deposited on the central portion of the nanocrystal to increase the percentage of (111) facets on the surface. Comparison of the intensity ratios of XRD peaks indicates that the transformation of shape resulted in a decrease in the proportion of higher energy (110) facets on the nanocrystals (see Supporting Information). As demonstrated for both Ag and Pd,[12] the oxygen in air plays a key role in the morphological evolution. Continuous bubbling of Ar during the synthesis greatly improved the stability of the branched Rh nanocrystals. Figure 2 shows TEM images of Rh nanocrystals that were obtained under Ar protection at $t = 10$ min and 48 h, respectively. From these images, it is apparent that the branched morphology could be

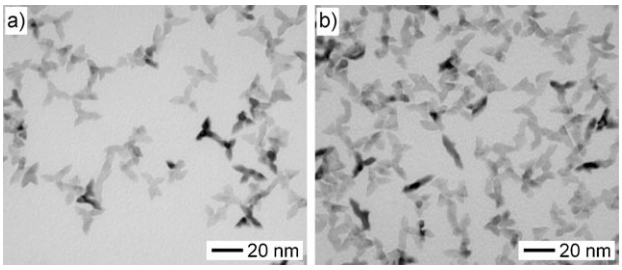

Figure 2. TEM images of Rh nanocrystals synthesized under Ar at 140 °C for a) 10 min and b) 48 h.

preserved for a long period of time when oxidative etching was excluded from the synthesis.

The UV/Vis absorption spectrum of the branched Rh nanocrystals displayed an attractive surface plasmon resonance (SPR) feature (Figure 3a); a weak and broad peak

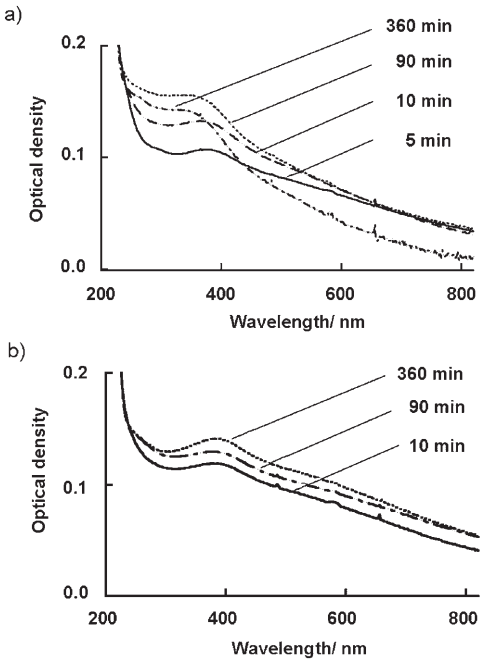

Figure 3. UV/Vis spectra of the Rh nanocrystals as a function of reaction time. The reaction was performed under a) air and b) continuous bubbling of Ar gas. Note that the surface plasmon resonance peak of the Rh multipods was shifted toward shorter wavelengths with increasing reaction time when air was present in the synthesis.

around 380 nm appeared in the initial stage of the reaction. It is well documented that both thin films and spherical nanoparticles of Rh do not exhibit any extinction peaks in the visible region as a result of the very small imaginary part of the dielectric constant.[13] To understand this optical feature, we carried out discrete dipole approximation (DDA) calculations for an individual Rh spherical particle of 10 nm diameter and a tripod nanocrystal featuring an outer triangle of 19 nm, a thickness of 5 nm, and an inner angle of 120° (see Supporting Information).[14] In general, if the geometric parameters are known, DDA calculations can predict the contributions of scattering and absorption to the extinction spectra as well as the peak positions. The calculations indicate that a spherical particle has an SPR peak in the deep UV region while the tripod displays a peak around 380 nm. Although the tripod was assumed to have a planar structure to save computational time, the DDA calculation nearly replicated the observed UV/Vis absorption spectrum of the branched Rh nanocrystals. The experimental spectrum displayed a somewhat broader resonance peak, which is most likely caused by the variation in both shape and size of the Rh nanocrystals in the real sample. In the presence of air, the SPR peak shifted toward shorter wavelengths as the reaction proceeded (Figure 3a). This shift can be attributed to the transformation from the branched shape into a spherical one. The spectral changes indicate that oxidative etching had already started at about 10 minutes into the reaction. In contrast, the position of the SPR peak remained unchanged over time (see Figure 3b) when the reaction was carried out under Ar. The peak gradually became more intense with the reaction time. This observation implies that protection by Ar not only promoted anisotropic growth but also helped to preserve the less stable, branched morphology.

We also systematically varied the reaction conditions to find the optimal parameters for generating branched Rh nanocrystals. In general, both the reaction temperature and the concentration of the precursor played important roles in determining the morphology of the product. As compared to the sample prepared at 140 °C, a decrease in the temperature (e.g., to 110 °C, Figure 4a) led to the formation of branched structures with higher aspect ratios (with arms ca. 2 nm wide by ca. 10–11 nm long). In contrast, relatively isotropic, cubelike nanocrystals were obtained at a higher temperature (180 °C, Figure 4b). When the reaction conditions were fixed at 140 °C and 10 min, a decrease in the concentration of Na_3RhCl_6 by five times (to 5 mM, Figure 4c) resulted in embryonic multipods that featured largely faceted rather than

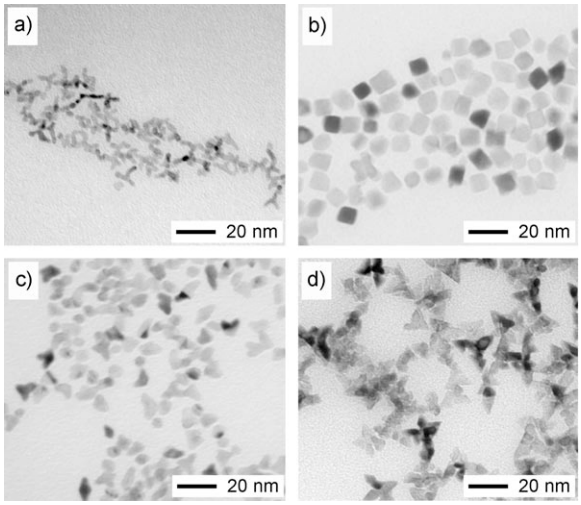

Figure 4. TEM images showing the effects of temperature and the concentration of the precursor on the formation of branched Rh nanocrystals: a) 25 mM Na_3RhCl_6 at 110 °C; b) 25 mM Na_3RhCl_6 at 180 °C; c) 5 mM Na_3RhCl_6 at 140 °C; and d) 50 mM Na_3RhCl_6 at 140 °C. All samples were collected at $t = 10$ min into the reaction.

spherical nanostructures. When the concentration of Na_3RhCl_6 was doubled (to 50 mM, Figure 4d), the branched morphology was also observed. Interestingly, the majority of these nanostructures were tetrapods rather than tripods.

As the thermodynamically favored particle shape of a face-centered-cubic metal is a truncated octahedron, the branched morphology must be a kinetically controlled product. The finding that anisotropic growth prevailed at relatively lower temperatures is consistent with the results that were recently obtained for Rh multipods synthesized through a different polyol process.[9b] Chen et al. proposed that the shape of a particle of gold (or another face-centered-cubic metal) is mainly determined by the competitive growth along the ⟨111⟩ and ⟨100⟩ directions.[7a] As the reaction temperature was increased, the rates of growth along these two directions were decreased to generate cubic nanocrystals. The shape of Rh nanocrystals was also strongly dependent on the concentration of the precursors. Although branched seeds were formed at all concentrations of Na_3RhCl_6 examined in the present work (5, 25, and 50 mM), TEM studies revealed no additional growth of the crystals and a drastic transformation of their shape with time in the case of 5 mM Na_3RhCl_6. These observations indicate that most of the precursor was consumed in the nucleation stage. In comparison, there was precursor left in the solution after nucleation when higher concentrations (e.g., 25 and 50 mM) of Na_3RhCl_6 were involved. As a result, the arms of each branched seed could continue to grow. As long as the difference in growth rate along the ⟨111⟩ and ⟨100⟩ directions was maintained, the branched nanocrystals could grow into larger dimensions without a change in their morphology.

The interesting plasmonic properties of these multipods may make them attractive for use as SERS substrates. One of the primary enhancement mechanisms in SERS is a result of electromagnetic enhancement arising from the extremely high local fields due to surface plasmon resonance (SPR).[15] Previous explorations of SERS on Group VIIIB metals such as Rh have suffered from fairly weak enhancement.[16] However, these studies have mainly focused on Rh-coated electrodes or Rh particles less than 10 nm in size, none of which exhibited any SPR features in the visible region. Figure 5 compares the SERS activities of thin films cast from three types of Rh nanocrystals: a) multipods synthesized under Ar, b) multipods synthesized in air, and c) nanocubes. The nanocubes of 9 nm in edge length exhibited a SPR peak at 250 nm, while the multipods showed SPR peaks at 360 nm and 380 nm for those synthesized in air and under Ar, respectively. We selected 4-mercaptopyridine (4-MP) as a probe molecule because it has a large scattering cross-section[17] and it has been well studied.[18] Using films that had been modified with 4-MP, it was found that both of the multipod samples gave well-defined, relatively strong SERS signals while the signal from the cubes was quite weak. The multipods prepared under Ar had the highest activity, with an enhancement that was 19 times stronger than that for the nanocubes. These results suggest a trend of stronger SERS signal with a red shift in the SPR peak. It is also possible that the sharp tips of the multipods provided additional enhancement. Recent studies have shown that nanoparticles with

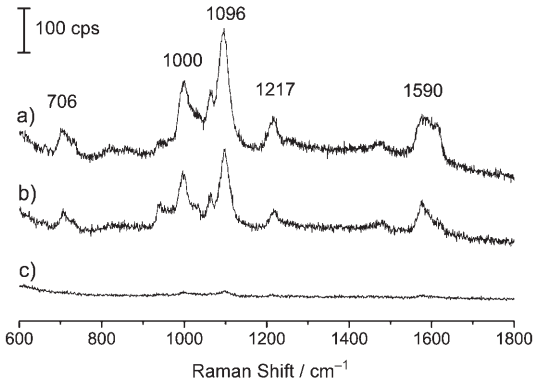

Figure 5. SERS spectra (cps = counts per second) of 4-mercaptopyridine on films of Rh nanocrystals: a) multipods synthesized under Ar (see Figure 2b); b) multipods synthesized in air (see Figure 1a); and c) 9-nm wide cubes (see Figure 4b).

sharp corners or edges are especially active SERS substrates, as the local value of $|E|^2$ at the tips can be more than 500 times that of the applied field.[19] While the SERS results shown here are purely qualitative, the high-quality spectra obtained with the Rh multipods are encouraging and may warrant further exploration.

In summary, we have demonstrated that Rh multipods can be prepared in large quantities by reducing Na_3RhCl_6 with ethylene glycol in the presence of PVP. These highly branched nanocrystals are not stable in air at elevated temperatures; they are slowly converted into spherical particles when the synthesis was allowed to proceed for long periods of time. We believe the formation of multipods is a kinetically controlled process, and thus parameters such as precursor concentration and temperature both play important roles in controlling the morphology of the product. When the synthesis was protected with continuous bubbling of Ar, both the anisotropy in growth and the stability of the product could be enhanced. The optical properties of the tripods were experimentally and theoretically investigated by UV/Vis spectroscopy and DDA calculations, with both methods indicating the presence of an SPR peak around 380 nm for the tripods. These Rh multipods display unprecedented SERS activities, which may find use in applications such as the in situ monitoring of catalytic reactions.[20]

Experimental Section

In a typical synthesis, ethylene glycol (EG; J. T. Baker; 2 mL) was placed in a three-necked flask equipped with a reflux condenser and a magnetic stirrer bar embedded in PYREX glass and heated in air at the designated temperature (e.g., 110, 140, or 180 °C) for 1.5 h. A temperature controller (ACE, 12125–14) equipped with a probe (ChemGlass, 104 TC105) and mantle heater (Electrothermal, HM0050-HS1) was used to maintain the temperature. In separate vials, Na_3RhCl_6 (34.6 mg, 9.0×10^{-2} mmol, Aldrich) and poly(vinyl pyrrolidone) (PVP; $M_r = 55\,000$, Aldrich; 51.3 mg, 4.5×10^{-1} mmol in terms of the repeating unit) were each dissolved in EG (0.8 mL) at room temperature. The molar ratio of Na_3RhCl_6 and the repeating unit of PVP was controlled at 1:5. These two solutions in EG were injected simultaneously into the heated EG using a syringe pump at a rate of 0.2 mL min^{-1}. All of the precursor was reduced to Rh

multipods, as indicated by UV/Vis spectroscopy. The reaction was continued up to 120 h. A set of samples was taken over the course of each synthesis using a glass pipette. For synthesis performed under Ar, all other experimental parameters were kept the same except for the continuous bubbling of Ar gas. The product was collected by centrifugation and washed with acetone and water several times to remove EG and excess PVP.

The as-obtained samples were characterized by transmission electron microscopy (TEM; JEOL 1200EX II, operated at 80 kV), powder X-ray diffraction (XRD; Philips 1820 diffractometer, $\lambda = 0.154180$ nm), and UV/Vis spectroscopy (Hewlett Packard 8452A diode-array spectrometer). TEM samples were prepared by placing a drop of the aqueous suspension on a carbon-coated copper grid (Ted Pella, Redding, CA), and drying under ambient conditions. The substrate for surface-enhanced Raman scattering (SERS) was prepared by drying a 3-μL aliquot of the final product on a 25-nm thick Al film supported on a Si wafer. The sample was then incubated in an aqueous solution of 4-mercaptopyridine (4 mM) for 1 h, rinsed with deionized water, and dried in air. SERS spectra were obtained with laser excitation (3 mW at the sample) at 785 nm (Renishaw HPNIR785 laser) and a spot size of approcimately 1.6 μm using a Leica DM IRBE optical microscope equipped with a Renishaw inVia Raman spectrometer and a thermoelectrically cooled CCD detector.

Received: September 7, 2005
Published online: January 17, 2006

Keywords: nanostructures · Raman spectroscopy · rhodium · surface plasmon resonance

[1] a) Y. Xia, P. Yang, Y. Sun, Y. Wu, B. Mayers, B. Gates, Y. Yin, F. Kim, H. Yan, *Adv. Mater.* **2003**, *15*, 353 – 389; b) Y. Xia, N. J. Halas, *MRS Bull.* **2005**, *30*, 338 – 348; c) Y. Sun, Y. Xia, *Science* **2002**, *298*, 2176 – 2179; d) E. C. Scher, L. Manna, A. P. Alivisatos, *Philos. Trans. R. Soc. London Ser. A* **2003**, *361*, 241 – 257; e) P. Yang, *MRS Bull.* **2005**, *30*, 85 – 91; f) C. J. Murphy, *Science* **2002**, *298*, 2139 – 2141.

[2] a) D. J. Milliron, S. M. Hughes, Y. Cui, L. Manna, J. Li, L.-W. Wang, A. P. Alivisatos, *Nature* **2004**, *430*, 190 – 195; b) D. L. Wang, C. M. Lieber, *Nat. Mater.* **2003**, *2*, 355 – 356.

[3] a) L. Manna, E. C. Scher, A. P. Alivisatos, *J. Am. Chem. Soc.* **2000**, *122*, 12700 – 12706; b) X. Peng, *Adv. Mater.* **2003**, *15*, 459 – 463; c) Z. A. Peng, X. Peng, *J. Am. Chem. Soc.* **2002**, *124*, 3343 – 3353.

[4] a) Y. W. Jun, S. M. Lee, N. J. Kang, J. Cheon, *J. Am. Chem. Soc.* **2001**, *123*, 5150 – 5151; b) M. Chen, J. Lu, S. Zhang, Y. Xie, Y. Xiong, Y. Qian, X. Liu, *J. Mater. Chem.* **2002**, *12*, 748 – 753.

[5] a) L. Manna, D. J. Milliron, A. Meisel, E. C. Scher, A. P. Alivisatos, *Nat. Mater.* **2003**, *2*, 382 – 385; b) C. Y. Yeh, Z. W. Lu, S. Froyen, A. Zunger, *Phys. Rev. B* **1992**, *46*, 10086 – 10097.

[6] C. Kittel, *Introduction to Solid State Physics*, 7th ed., Wiley, New York, **1996**.

[7] a) S. Chen, Z. L. Wang, J. Ballato, S. H. Foulger, D. Carroll, *J. Am. Chem. Soc.* **2003**, *125*, 16186 – 16187; b) E. Hao, R. C. Bailey, G. C. Schatz, J. T. Hupp, S. Li, *Nano Lett.* **2004**, *4*, 327 – 330.

[8] a) J. Chen, T. Herricks, Y. Xia, *Angew. Chem.* **2005**, *117*, 2645 – 2648; *Angew. Chem. Int. Ed.* **2005**, *44*, 2589 – 2592; b) T. Herricks, J. Chen, Y. Xia, *Nano Lett.* **2004**, *4*, 2367 – 2371; c) X. Teng, H. Yang, *Nano Lett.* **2005**, *5*, 885 – 891.

[9] a) H. Hirai, Y. Nakao, N. Toshima, *J. Macromol. Sci. Chem. A* **1978**, *12*, 1117 – 1141; b) J. D. Hoefelmeyer, K. Niesz, G. A. Somorjai, D. Tilley, *Nano Lett.* **2005**, *5*, 435 – 438.

[10] We were unable to synthesize well-defined Rh multipods when $RhCl_3 \cdot n H_2O$ was used as a precursor. Water seems to enhance oxidative etching and thus greatly modify the shape of a nanocrystal.

[11] Q. Jiang, H. M. Lu, M. Zhao, *J. Phys. Condens. Matter* **2004**, *16*, 521 – 530.

[12] a) B. Wiley, T. Herricks, Y. Sun, Y. Xia, *Nano Lett.* **2004**, *4*, 1733 – 1739; b) Y. Xiong, J. Chen, B. Wiley, Y. Xia, S. Aloni, Y. Yin, *J. Am. Chem. Soc.* **2005**, *127*, 7332 – 7333.

[13] Y. Wang, S. D. Russell, R. L. Shimabukuro, *J. Appl. Phys.* **2005**, *97*, 023708.

[14] a) B. T. Drani, P. J. Flatau, *J. Opt. Soc. Am. A* **1994**, *11*, 1491 – 1499; b) R. Jin, Y. Cao, C. A. Markin, K. L. Kelly, G. Schatz, J.-G. Zheng, *Science* **2001**, *294*, 1901 – 1903; c) Y. Xiong, J. Chen, B. Wiley, Y. Xia, Y. Yin, Z.-Y. Li, *Nano Lett.* **2005**, *5*, 1237 – 1242.

[15] N. Halas, *MRS Bull.* **2005**, *30*, 362 – 367.

[16] Z.-Q. Tian, B. Ren, D.-Yin. Wu, *J. Phys. Chem. B* **2002**, *106*, 9463 – 9482.

[17] W. B. Cai, B. Ren, X. Q. Li, C. X. She, F. M. Liu, X. W. Cai, Z. Q. Tian, *Surf. Sci.* **1998**, *406*, 9 – 22.

[18] Z. Wang, S. Pan, T. D. Krauss, H. Du, L. J. Rothberg, *Proc. Natl. Acad. Sci. USA* **2003**, *100*, 8638 – 8643.

[19] K. L. Kelly, E. Coronado, L. L. Zhao, G. C. Schatz, *J. Phys. Chem. B* **2003**, *107*, 668.

[20] R. Gomez, J. Perez, J. Solla-Gullon, V. Montiel, A. Aldaz, *J. Phys. Chem. B* **2004**, *108*, 9943 – 9949.

